HHS Public Access

Author manuscript

J Safety Res. Author manuscript; available in PMC 2024 September 01.

Published in final edited form as:

J Safety Res. 2023 September ; 86: 5–11. doi:10.1016/j.jsr.2023.05.014.

VALIDATION OF A PORTABLE SHOE TREAD SCANNER TO PREDICT SLIP RISK

Sarah L Hemler[a,b,c], **Kurt E. Beschorner**[a]

[a]Department of Bioengineering, University of Pittsburgh, Pittsburgh, PA; USA

[b]Faculty of Medicine, University of Geneva, Geneva, Switzerland

[c]Unit of Therapeutic Patient Education, WHO Collaborating Centre, Geneva University Hospitals, Geneva, Switzerland

Abstract

Problem: Worn shoes are an important contributor to occupational slip and fall injuries. Tools to assess worn tread are emerging; imaging tools offer the potential to assist. The aim of this study was to develop a shoe tread scanner and evaluate its effectiveness to predict slip risk.

Methods: This study analyzed data from two previous studies in which worn or new slip-resistant shoes were donned during an unexpected slip condition. The shoe tread for each shoe was scanned using a portable scanner that utilized frustrated total internal reflection (FTIR) technology. The shoe tread parameters of the worn region size (WRS) for worn shoes and total contact area for new shoes were measured. These parameters were then used to predict slip risk from the unexpected slip conditions.

Results: The WRS was able to accurately predict slip risk, but the contact area was not.

Discussion: These findings support that increased WRS on the shoe outsole is associated with worse slip outcomes. Furthermore, the tool was able to offer robust feedback across a wide range of tread designs, but the results of this study show that the tool may be more applicable for slip-resistant shoes that are worn compared to their new counterparts.

Summary: This study shows that FTIR technology utilized in this tool may be a useful and portable method for determining slip risk for worn shoes.

Practical Applications: This tool has the potential to be an efficient, objective, end-user tool that improves timely replacement of shoes and prevention of injuries.

Keywords

Slips, trips, and falls; frustrated total internal reflection (FTIR); Footwear; risk assessment tools

Corresponding author: Sarah Hemler sarah.hemler@unige.ch.

Competing Interest

The authors have no competing interests with the work described in this manuscript.

1. Problem

Slips, trips, and falls are a leading cause of occupational injury. In the United States, slips, trips, and falls account for about 28% of all nonfatal occupational injuries (U.S. Department of Labor - Bureau of Labor Statistics, 2021). Twenty-five to 50% of same-level falls are due to slipping (Courtney et al., 2001; U.S. Department of Labor - Bureau of Labor Statistics, 2022) with slipping largely due to insufficient friction at the shoe-floor interface (Hanson et al., 1999).

Footwear outsole design is an important aspect for reducing the prevalence of slips and falls. Specifically, the design of shoe outsole tread has the potential to improve shoe-floor friction and under-shoe fluid drainage (traction performance) (Beschorner et al., 2014; Hemler, Pliner, et al., 2020). Shoes labeled as slip-resistant (SR) often have treaded regions that are often separated by channels; the separated sections are often referred to as tread blocks. These channels allow for fluid to be dispersed from under the shoe if an individual steps on a contaminated surface. However, when the tread blocks are worn down to the same depth as the channels, the fluid can become trapped and pressurized under the shoe (Beschorner et al., 2014). This fluid pressurization under the shoe leads to increased slip risk (Beschorner et al., 2014). The continuous region on the shoe tread that lacks tread channels either due to design or progressive shoe wear, has been termed the worn region size (WRS). Research has shown that as shoes are worn, this WRS grows, which leads to decreases in traction performance and increases in slip risk (Beschorner et al., 2020; Hemler et al., 2019; Hemler et al., 2022; Sundaram et al., 2020).

Lubrication theory can explain the relationship between tread geometry of new and worn shoes, and slip risk. Calculations for the predicted film thickness between the two surfaces separated by a fluid incorporate contaminant characteristics in addition to the dimensions of the worn region or a single tread block if no worn region has developed (Fuller, 1956). For new SR shoes, the smaller tread block size leads to a low film thickness that is associated with boundary lubrication where the contacting asperities dominate friction and the fluid film effects are negligible (Hemler, Charbonneau, et al., 2020; Stachowiak & Batchelor, 2013). However, as the WRS grows, the film thickness increases leading to a change in the lubrication regime and associated decrease in friction (Hemler, Charbonneau, et al., 2020). This region where there is a change to the mixed lubrication regime and then to the hydrodynamic lubrication region is where slips are more likely to occur. As such, worn shoes that generally have larger continuous regions of tread are more likely to lead to higher slip risk (Hemler et al.; Hemler et al., 2022; Sundaram et al., 2020).

Current methods for assessing shoe slip risk of shoes are either inappropriate or impractical for regularly assessing the worn condition. Shoe friction testing devices are often used to measure the available coefficient of friction between a shoe and flooring (Aschan et al., 2005; Iraqi, Cham, Redfern, & Beschorner, 2018; Wilson, 1996). These tribometers offer accurate, biomimetic measurements for a variety of contaminant-shoe-floor combinations, yet often are costly, require extensive training, and do not adapt to changes in frontal plane angle due to asymmetric shoe wear. Other methods for assessing shoe safety rely on

qualitative recommendations such as “when the shoe is too worn,” or on tools measuring the tread depth (Shoes For Crews, 2019). These metrics are good for providing a general threshold for wear, however, this benefit may be undermined by individual subjectivity. Furthermore, a metric such as tread depth has been shown to be an inadequate measure of friction changes due to wear (Grönqvist, 1995; Hemler et al., 2019). Recently, a method for assessing shoe slip risk was created that applies a common, household object (i.e., a battery) to the continuous worn region on a shoe (Beschorner et al., 2020). This method offers a simple and universally consistent method for determining the safety of shoes. However, this method was only tested for worn, SR shoes and requires user training. While existing methods are appropriate for assessing worn shoes in certain situations, there is a need for a tool that is easy-to-use, objective, automated, and predictive of slip risk for new and worn SR shoes.

As previous research has identified a distinct relationship between WRS and slip risk (Sundaram et al., 2020), there is large potential to create a tool that measures WRS to predict slip outcome. One potential method for detecting WRS is a technology called Frustrated Total Internal Reflection (FTIR). FTIR is a method for measuring the regions of contact on a transparent material; it describes the process of shining light into a transparent plate (waveguide) at an incident angle larger than the critical angle, which ensures the light is internally reflected when contacted by air (Needham & Sharp, 2016). The boundary condition changes when materials with a larger refractive index than air, such as shoe outsoles or skin, encounter the waveguide. The change enables light to be transmitted out of the waveguide, into the shoe outsole or skin, and then scattered. The scattered light illuminates the contact region, which can then be detected by a camera. While FTIR technology has been used for several centuries and for applications including footwear (Newton, 1952; Zhu et al., 1986), it has not yet been used to quantify the degree of wear on shoes.

In the case of new shoes, another friction mechanism dominates that can be targeted with FTIR measurements. Particularly, the friction of new slip-resistant shoes depends on the tread surface area (Jones et al., 2018). This previous research also identified other factors that influence the contact area like the shape of the heel (beveled versus flat) and the hardness of the material, which have also been associated with coefficient of friction. Prior research has determined that contact area is a relevant factor in boundary lubrication because it reduces contact pressure and increases hysteresis friction (Iraqi et al., 2020; Moghaddam, 2018). Similarly, other studies have demonstrated that other factors that influence the contact area such as the bending stiffness of tread also contribute to friction performance (Yamaguchi et al., 2017). Notably, the effect of contact area on friction performance does not extend to non-slip-resistant shoes because lack of drainage channels for some of these shoes leads to fluid pressures that cause these shoes not to be in the boundary lubrication (Meehan et al., 2022). Given the role of contact area on shoe-floor friction, FTIR may also provide reasonable predictions of slip risk for new slip-resistant shoes.

The aim of this study was to develop a tool using FTIR technology to identify the heel contact geometry on SR shoes. The secondary aim was to assess the ability of the tool to predict slips based on the measured heel contact geometry.

2. Methods

2.1. Summary

Worn and new SR shoes from two human slipping studies (*WornSlip* and *NewSlip*, respectively) were used in this analysis. Data from *WornSlip* have been previously reported (Sundaram et al., 2020). The procedures and part of the data from *NewSlip* have been presented (Beschorner et al., 2023). Thus, the methods from these two studies are only briefly summarized in this study. The shoe slipping studies consisted of exposing participants to an unexpected slippery condition. Slip outcome was collected for each study. The heels of the shoes were imaged on a shoe tread scanner. The largest WRS on worn shoes (*WornSlip*) and the total contact area (CA) for new shoes (*NewSlip*) was scanned, quantified, and related to the slip outcome.

2.2. Worn Shoe Slipping Study (WornSlip)

Fifty-seven participants took part in this experiment while wearing their own naturally worn shoes. Only shoes that were classified as slip-resistant by the manufacturer were included in our analysis (n=36). Participants were outfitted in tight-fitting clothing and a set of 79 reflective markers (Moyer, 2006) while they walked over laminate flooring. After a series of dry walking trials, the participant unexpectedly walked over a contaminated surface (100 mL of a 90% glycerol-10% water by volume solution). The anterior-posterior and medial-lateral positioning components of the inferior heel marker were used to calculate the slip speed using numerical differentiation (Cham & Redfern, 2002). The peak slip speed (PSS) was calculated as the local maximum speed at least 50 ms after heel contact. A step was identified as a slip if the PSS exceeded 0.2 m/s. This classification was based on previous research that found a bimodal distribution for slips with low-severity slips of fully treaded shoes below this cutoff and high-severity slips with untreaded shoes above this cutoff (Beschorner et al., 2014). Therefore, a PSS exceeding 0.2 m/s was designated as the cutoff variable for a slip. A detailed description of the study can be found in the full manuscript (Sundaram et al., 2020).

2.3. New Shoe Slipping Study (NewSlip)

Two slipping studies similar to *WornSlip* were conducted (Beschorner et al., 2023). As the methods across these two studies were identical for the participants that were included in this analysis, they are classified as one study in this analysis (*NewSlip*). A total of 38 participants wore new SR shoes. These shoes were designated as “slip-resistant” by their manufacturer and were collected from a curated list of different brands. The shoes were randomized to be given to the participants according to their reported gender and shoe size. If the shoes on the list were discontinued as in some cases, a similar shoe replacement was used. While donning the shoes, participants walked over tile flooring for several dry walking trials. Then, they were exposed to an unexpected slippery condition (250 mL of canola oil). Only the flooring and contaminant vary from the *WornSlip* study; all other methods are identical. The peak slip speed (PSS) and corresponding slip outcome were calculated in a similar manner to *WornSlip*.

2.4. Shoe Tread Scanner

2.4.1. Construction—The shoe tread scanner was created using a custom developed FTIR imaging device, a frame, and a camera (Figure 1). Materials consists of a light source (HitLights, 36in, 5050 LED), a waveguide (Americanflat Acrylic Picture Frame – 6in x 8in), and extruded t-slot aluminum (80/20, Inc., Columbia City, IN). The camera (GoPro Hero 3+, GoPro, Inc., San Mateo, CA, USA) sits on the base of the prototype under the platform. The framing allows for the waveguide to sit at angles adjustable from about 2–17°. The frame is strong enough to hold the full weight of an average individual. This system is portable (mass: 2.34 kg; dimensions: 26 cm × 22 cm × 20 cm) and the materials cost less than $200 USD.

2.4.2. Data Collection—Shoes from *WornSlip* and *NewSlip* were imaged on the shoe tread scanner. Two of the 36 pairs from *WornSlip* and 1 of the 38 pairs from *NewSlip* could not be located to be scanned. Additionally, four participants were excluded from *NewSlip* for not stepping on the contaminant or for seeing the contaminant prior to stepping on it. Thus, 34 and 33 shoes are included for the analyses for *WornSlip* and *NewSlip*, respectively. The scanner was set up to have a normal force of 75 lbf (334 N) applied via an apparatus that stably positioned 3, 25 lbf weights to the shoe. A sagittal plane angle of 7° was also utilized (Figure 2). This angle was chosen for two primary reasons. At an angle of 7°, more of the worn regions of the outsole were visible than at higher angles (Iraqi, Cham, Redfern, Vidic, et al., 2018). In preliminary analyses, the size of these visible regions were more consistent with the posterior 50 mm of the shoe heel that has previously been identified to contribute to shoe-floor friction and lubrication behavior (Iraqi et al., 2020; Jones et al., 2018; Singh & Beschorner, 2014). Second, although previous research has shown that angles larger than 7° are associated with the onset of slipping (Iraqi, Cham, Redfern, Vidic, et al., 2018), a rotational moment is created by the frictional forces during a slip that may rotate a portion of the heel to better conform with the floor. A shallower angle may be appropriate for reproducing this phenomenon.

Worn shoes from *WornSlip* were rotated along the frontal plane (i.e., inversion or eversion) to capture the largest worn region on the shoe. This technique was employed to simulate as if a person was standing on the scanner and was asked to shift body weight back and forth so that the most worn region could be identified by the scanner. The shoes from *NewSlip* were not rotated since they did not have a worn region.

2.4.3. Image Processing—The raw images from the scanner camera were processed in a series of steps to obtain the area of the largest continuous worn region on shoes (Figure 3). Raw images of the shoe-waveguide contact were captured by a camera with a wide-angle lens (GoPro Hero 3+, GoPro, Inc., San Mateo, CA, USA). The 7MP Medium mode for the still images was used (Figure 3, step A). A custom algorithm (MATLAB® R2020a, Natick, Massachusetts: The MathWorks Inc.) was used to apply a series of steps to analyze the images. After the raw image was imported, a calibration function was used to flatten the wide-angle image using a checkerboard with 9×10 blocks each with checkered block side lengths of 11.4 mm (Figure 3, step B). The image was cropped by the user to select the portion of the image containing the tread in contact with the waveguide (Figure 3, step C).

The contact regions were determined by the user selecting two of the brightest and dullest features of the contact regions (Bharthi et al., 2022). Within those four points, the minimum and maximum hue, saturation, and brightness that were measured were used to define the range for these parameters for identifying contact pixels. Of a possible range from 0–1 for each parameter, a buffer value of 0.05 was added to the maximum value and subtracted from the minimum value to increase, by 10%, the range which was used to determine the contact regions on the image (Figure 3, step D). Connected pixel components were identified so that the largest continuous regions were identified and quantified (Figure 3, step E). The calibration board from step 1 was used to determine the size of the pixels closest to the largest contact regions (Figure 3, step F). This pixel-to-area conversion was then applied to convert the number of pixels to the size of the largest contact regions (Figure 3, step G). The methods described were also performed to determine the largest contact area for the *NewSlip* shoes with steps 4 and 6 removed since contact area includes all contact region and does not require identifying the largest contact region. This image processing technique was verified to produce accurate results by using tread blocks of known sizes on multiple shoes. This technique was able to identify the size of the tread blocks within 8–18% accuracy (Hemler, 2021).

2.4.4 Statistical Analyses—Multiple models were used to assess the ability of the scanner to predict slip outcome. Two univariate logistic regression analyses were used to assess the ability of the tool to predict slip risk based on FTIR data. Specifically, one logistic regression was used to assess the ability of the WRS (independent variable) of worn SR shoes from *WornSlip* to predict slip outcome (dependent variable). Another logistic regression assessed the ability of total CA (independent variable) of the new shoes from *NewSlip* to predict slip outcome (dependent variable).

In all models the WRS was square-root transformed to normalize residuals. Previous work has showed an increase in slip risk associated with increased shoe wear (Beschorner et al., 2014). Therefore, one-tailed analyses were used for all models such that increasing WRS and CA would be associated with increasing slip risk. All statistical analyses were determined prior to performing the tests via Stata/SE (Stata/SE 15, StataCorp, College Station, TX).

3. Results

The WRS across all *WornSlip* shoes ranged from 1–1006 mm^2 with a mean (SD) of 133.4 (224.3) mm^2 (Table 1). The mean (SD) WRS for shoes that slipped and did not slip were 214.8 (284.9) mm^2 and 30.3 (34.0) mm^2, respectively. Nineteen of the 34 participants in *WornSlip* slipped with a mean (SD) peak slipping speed of 0.77 (0.71) m/s and range of 0.21–2.63 m/s.

The total contact area (CA) across all *NewSlip* shoes ranged from 306.0–1046.0 mm^2 with a mean (SD) of 601.9 (203.0) mm^2 (Table 1). The mean (SD) CA for shoes that slipped and did not slip were 598.6 (196.0) mm^2 and 604.9 (215.5) mm^2, respectively. Sixteen of the 33 participants in *NewSlip* slipped with a mean (SD) peak slipping speed of 0.83 (0.75) m/s and range of 0.21–2.98 m/s.

The model for *WornSlip* showed that the WRS was able to significantly predict slip outcome ($\chi^2_{(1, n=34} = 11.3$, $p = 0.043$) (Figure 4). Slip risks of 50% and 80% were associated with worn region sizes of 54 mm^2 and 140 mm^2, respectively. The odds ratio for slipping is 5.0 for every 100 mm^2 increase in WRS. The model for *NewSlip* showed that the total CA was not able to significantly predict slip outcome ($\chi^2_{(1, n=33} = 0.01$, $p = 0.928$) (Figure 5).

4. Discussion

This study shows that the portable shoe tread scanner presented in this study can be used as an objective, end-user tool that predicts slipping outcome from the measured WRS of the shoe outsole. The tool predicted slips for worn shoes using the WRS, but not for new SR shoes using contact area.

The development of this tool aligns with previous methods and expands upon previous findings. Previous work found that WRS, when measured using methods different than the present study, is associated with under-shoe fluid pressures and slip severity (Hemler et al., 2019; Hemler, Pliner, et al., 2020). The present study demonstrated consistency with these prior studies. Furthermore, previous methods that developed a dichotomous metric of worn condition, by comparing the worn region to a AA and AAA battery (Beschorner et al., 2020), also found that a larger WRS is consistent with increased under-shoe fluid pressures, decreased friction, and increased slip severity (note that the slip severity data from this prior study is the same data set as the present study). Thus, this research adds to a growing body of evidence that increased size of the worn region is associated with worse slip outcomes regardless of the metric used to quantify the worn region.

Based on the findings from this work, this scanner could offer robust feedback across a wide range of tread designs. The tread pattern of the shoes varied with some having small tread blocks and others having large and long tread blocks. Also, the shoe tread blocks varied in color. For example, one shoe had multi-colored, marbled tread. The image processing technique was able to accurately identify the tread regions in contact across these types of shoe tread (Figure 6). The effective scanning of these shoes provides evidence that shoes with designs atypical to traditional SR, and potentially non-SR shoes may work well on the tool.

Thresholds for wear may be dependent on the tool used to define the WRS. The tool in this study generally identified WRSs that were smaller than the entire continuous worn region on the shoe as measured using calipers in previous work (Sundaram et al., 2020). Upon observing this difference, the authors conducted a post-hoc analysis to compare the worn region size measured by the FTIR device in the present study to the worn region size measured with calipers from the prior study (Sundaram et al., 2020). As mentioned, both the tool and human slipping study accurately predicted slip risk based on their measured WRS. A bivariate correlation analysis between the square-root transformed worn region measurements showed a strong correlation between these two methods ($R = 0.69$, $t_{32} = 5.4$, $p < 0.001$, $\sqrt{caliper} = 1.4(\sqrt{FTIR} + 11.2)$), showing that these methods are associated and relatable. The present study and prior study lead to different cutoff values associated with a slipping risk of 50%, 80%, and 95% (Table 2). Therefore, it is important to note that these

two methods of measuring the WRS – the present tool or from calipers as in the previous study – may provide different slip risk thresholds that are accurate within each respective method and are comparable with a scaling factor.

For new shoes, the contact area did not directly describe the risk of slipping. There may be multiple reasons for this finding. Previous research has shown that increased contact area leads to higher coefficient of friction (COF) (Jones et al., 2018; Moghaddam et al., 2018), which is due to decreased contact pressures at the shoe-floor interface (Moghaddam et al., 2018). However, previous work has also shown that combining multiple factors of shoes such as contact area, hardness, heel shape, and flooring, best describes the traction of the shoes (Iraqi et al., 2020). In the current study, as only contact area was measured, there may be important variables from other parameters such as hardness, heel shape, and flooring that influence the risk of slipping and could be included in future analyses. Lastly, evidence suggests that the effect size of contact area on COF may be lower than the effect of worn region size on COF. Notably, going from the first to third quartile of contact area results in a 20% increase in COF (Iraqi et al., 2020), while reducing the worn region size (third quartile to first quartile) resulted in a 58% increase in COF. Therefore, this tool may be more appropriate for SR shoes that have been worn compared to new SR shoes.

Certain limitations of the tool should be considered. The camera used in this study had a color-correcting function that resulted in the scans appearing to have one of three filter shades – black, blue, or purple. The filter associated with the blue color did not contrast well with black tread and required detailed manual processing. Future tool development might include a camera with consistent image coloring that would eliminate this limitation. Furthermore, four shoes from *WornSlip* had fine surface texturing that may have inhibited detection of the worn region as one continuous area. However, these shoes were not outliers within the models, which suggests the texturing does not affect the accuracy of the model. As the shoes were loaded on the scanner, angles along the frontal plane of the shoe (inversion/eversion) were applied to best capture the largest region of wear at the specified sagittal plane angle of 7°. Due to the constraints of the apparatus, however, the largest worn region could not always be fully captured. As such, future work may develop a method to capture the worn regions across the heel portion or entire outsole of the shoe. It should be noted that the contaminants used in *WornSlip* and *NewSlip* varied and could have influenced the slip outcome measures. Future work should analyze the efficacy of the tool to predict slips across a variety of contaminants. Lastly, user training is currently required to operate the tool; future development will reduce the role of the user and associated training required to make the tool an efficient, objective, end-user tool.

5. Summary

This study showed that a portable shoe tread scanner utilizing FTIR technology could be used to scan shoes and give an accurate prediction of slip outcome. This tool may be especially useful for worn, SR shoes. Furthermore, this tool may guide thresholds for slip risk assessment in conjunction with other tools that assess the worn conditions (e.g., battery test, measuring worn region with calipers).

6. Practical Applications

There is an opportunity that with future development, this tool can be an efficient, objective, end-user tool across multiple industries. Service industries, often requiring employees to wear SR shoes, and the corresponding insurance companies could benefit from the tool for timely replacement of shoes and prevention of injuries. Incorporating this tool into routine use would improve timely replacement of shoes and would improve employee awareness of the need for shoe monitoring and replacement. Particularly, the future automation (to replace the user-selected contact regions) in addition to the portability of the tool are two aspects that would make the tool attractive for industries where time and resources are limited (e.g., fast food restaurants). To achieve this potential, continued and sustained development is needed to translate the device from a laboratory setting to workplace environments. Furthermore, the tool validation could be expanded and quantitative thresholds for wear could be set providing a useful tool to end-users.

Acknowledgements

This research was funded by the National Institute on Aging (R44 AG059258), National Institute for Occupational Safety and Health (NIOSH R01 OH 010940), National Science Foundation (NSF GRFP 174752), National Institute for Occupational Safety and Health (R03ActOH011069), and National Center for Research Resources (NCRR S10RR027102).

Biographies

Sarah Hemler, Ph.D., is a Postdoctoral fellow at the University of Geneva and Geneva University Hospitals in Geneva, Switzerland. Her main research goals include preventing injury across multiple domains and populations with her most recent work covering occupational slip and fall prevention and creating intelligent footwear for preventing lower-limb amputation in people with diabetes. She received her B.S. in Mechanical Engineering from the University of Maryland, Baltimore County, and her PhD in Bioengineering at the University of Pittsburgh as an NSF Graduate Research Fellow.

Kurt Beschorner, Ph.D., is an Associate Professor of Bioengineering at the University of Pittsburgh. His research mission is to apply core competencies in tribology, biomechanics, and ergonomics to prevent falling accidents. He received his B.S. in Mechanical Engineering from the University of Illinois Urbana-Champaign and his Ph.D. in Bioengineering from the University of Pittsburgh.

7. References

Aschan C, Hirvonen M, Mannelin T, & Rajamäki E (2005). Development and validation of a novel portable slip simulator. Applied ergonomics, 36(5), 585–593. [PubMed: 15970203]

Beschorner KE, Albert DL, Chambers AJ, & Redfern MS (2014). Fluid pressures at the shoe–floor–contaminant interface during slips: Effects of tread & implications on slip severity. Journal of Biomechanics, 47(2), 458–463. [PubMed: 24267270]

Beschorner KE, Chanda A, Moyer BE, Reasinger A, Griffin SC, & Johnston IM (2023). Validating the ability of a portable shoe-floor friction testing device, NextSTEPS, to predict human slips. Applied ergonomics, 106, 103854. [PubMed: 35973317]

Beschorner KE, Siegel JL, Hemler SL, Sundaram VH, Chanda A, Iraqi A, Haight JM, & Redfern MS (2020). An observational ergonomic tool for assessing the worn condition of slip-resistant shoes. Applied ergonomics, 88, 103140. [PubMed: 32678768]

Bharthi R, Sukinik JR, Hemler SL, & Beschorner KE (2022). Shoe Tread Wear Occurs Primarily during Early Stance and Precedes the Peak Required Coefficient of Friction. Footwear Science, 1–10. [PubMed: 37701063]

Cham R, & Redfern MS (2002). Changes in gait when anticipating slippery floors. Gait & posture, 15(2), 159–171. [PubMed: 11869910]

Courtney TK, Sorock GS, Manning DP, Collins JW, & Holbein-Jenny MA (2001). Occupational slip, trip, and fall-related injuries–can the contribution of slipperiness be isolated? Ergonomics, 44(13), 1118–1137. [PubMed: 11794761]

Fuller D (1956). Theory and Practice of Lubrication for Engineers. John Wiley & Sons, Inc.

Grönqvist R (1995). Mechanisms of friction and assessment of slip resistance of new and used footwear soles on contaminated floors. Ergonomics, 38(2), 224–241. [PubMed: 28084937]

Hanson JP, Redfern MS, & Mazumdar M (1999). Predicting slips and falls considering required and available friction. Ergonomics, 42(12), 1619–1633. [PubMed: 10643404]

Hemler SL (2021). Mechanics and Assessment of Shoe Tread Wear – Replacement Strategies for Preventing Slips University of Pittsburgh].

Hemler SL, Charbonneau DN, & Beschorner KE (2020). Predicting hydrodynamic conditions under worn shoes using the tapered-wedge solution of Reynolds equation. Tribology International, 106161.

Hemler SL, Charbonneau DN, Iraqi A, Redfern MS, Haight JM, Moyer BE, & Beschorner KE (2019). Changes in under-shoe traction and fluid drainage for progressively worn shoe tread. Applied ergonomics, 80, 35–42. [PubMed: 31280808]

Hemler SL, Pliner EM, Redfern MS, Haight JM, & Beschorner KE (2020). Traction performance across the life of slip-resistant footwear: preliminary results from a longitudinal study. Journal of Safety Research.

Hemler SL, Pliner EM, Redfern MS, Haight JM, & Beschorner KE (2022). Effects of natural shoe wear on traction performance: a longitudinal study. Footwear Science, 1–12. [PubMed: 37701063]

Iraqi A, Cham R, Redfern MS, & Beschorner KE (2018). Coefficient of friction testing parameters influence the prediction of human slips. Applied ergonomics, 70, 118–126. [PubMed: 29866300]

Iraqi A, Cham R, Redfern MS, Vidic NS, & Beschorner KE (2018). Kinematics and kinetics of the shoe during human slips. Journal of Biomechanics, 74, 57–63. [PubMed: 29759653]

Iraqi A, Vidic NS, Redfern MS, & Beschorner KE (2020). Prediction of coefficient of friction based on footwear outsole features. Applied ergonomics, 82, 102963. [PubMed: 31580996]

Jones TG, Iraqi A, & Beschorner KE (2018). Performance testing of work shoes labeled as slip resistant. Applied ergonomics, 68, 304–312. [PubMed: 29409649]

Meehan EE, Vidic N, & Beschorner KE (2022). In contrast to slip-resistant shoes, fluid drainage capacity explains friction performance across shoes that are not slip-resistant. Applied ergonomics, 100, 103663. [PubMed: 34894586]

Moghaddam SRM (2018). Computational Models for Predicting Shoe Friction and Wear University of Pittsburgh].

Moghaddam SRM, Acharya A, Redfern MS, & Beschorner KE (2018). Predictive multiscale computational model of shoe-floor coefficient of friction. Journal of Biomechanics, 66, 145–152. [PubMed: 29183657]

Moyer BE (2006). Slip and fall risks: Pre-slip gait contributions and post-slip response effects University of Pittsburgh].

Needham JA, & Sharp JS (2016). Watch your step! A frustrated total internal reflection approach to forensic footwear imaging. Scientific reports, 6, 21290. [PubMed: 26880687]

Newton I (1952). Opticks, or, a treatise of the reflections, refractions, inflections & colours of light. Courier Corporation.

Shoes For Crews. (2019). Outsole Care. In.

Singh G, & Beschorner KE (2014). A Method for Measuring Fluid Pressures in the Shoe–Floor–Fluid Interface: Application to Shoe Tread Evaluation. IIE Transactions on Occupational Ergonomics and Human Factors, 2(2), 53–59. [PubMed: 31106007]

Stachowiak G, & Batchelor AW (2013). Engineering Tribology. Elsevier Science & Technology. http://ebookcentral.proquest.com/lib/pitt-ebooks/detail.action?docID=1402495

Sundaram VH, Hemler SL, Chanda A, Haight JM, Redfern MS, & Beschorner KE (2020). Worn Region Size of Shoe Outsole Impacts Human Slips: Testing a Mechanistic Model. Journal of Biomechanics, 105(109797).

U.S. Department of Labor - Bureau of Labor Statistics. (2021). Nonfatal Occupational Injuries and Illnesses Requiring Days Away From Work, 2019 (CSU00X4XXXXX6E000). https://www.bls.gov/data/home.htm

U.S. Department of Labor - Bureau of Labor Statistics. (2022). Nonfatal Occupational Injuries and Illnesses Requiring Days Away From Work, 2020 (CSU00X4XXXXX6E000,CSU00X422XXX6E000). https://www.bls.gov/data/home.htm

Wilson M (1996). Slip resistance characteristics of footwear solings assessed using the SATRA friction tester. Journal of Testing and Evaluation, 24(6), 377–385.

Yamaguchi T, Katsurashima Y, & Hokkirigawa K (2017). Effect of rubber block height and orientation on the coefficients of friction against smooth steel surface lubricated with glycerol solution. Tribology International, 110, 96–102.

Zhu S, Yu A, Hawley D, & Roy R (1986). Frustrated total internal reflection: A demonstration and review. American Journal of Physics, 54(7), 601–607.

Highlights:

- There is a lack of an objective, end-user tool for evaluating shoe tread to prevent slips.
- A shoe tread scanner was developed which utilizes Frustrated Total Internal Reflection technology
- The scanner captured the heel tread geometry from 57 worn and 38 new SR shoes.
- The region of wear on the worn shoes was able to predict slip risk, validating the tool
- Contact area of new shoes was not associated with slipping risk.

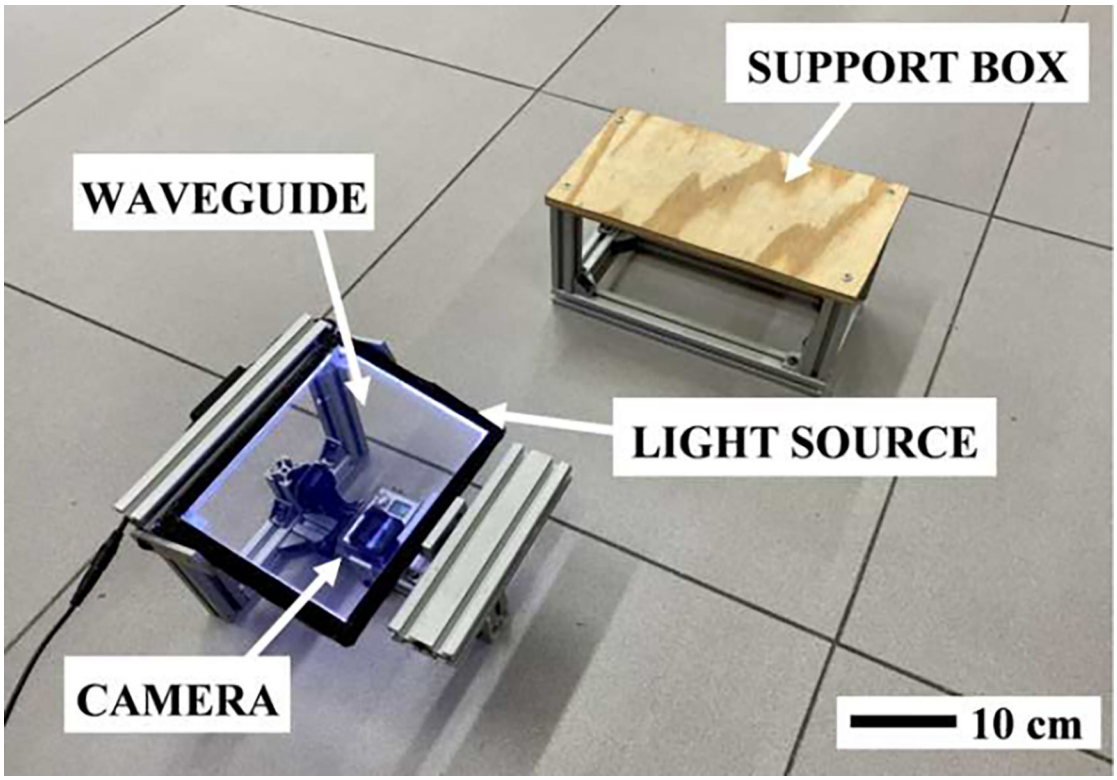

Figure 1.
Shoe Tread Scanner
The frame, waveguide, camera (below the waveguide), and light source can be seen on the left side of the figure. The support for the other foot is seen on the right.

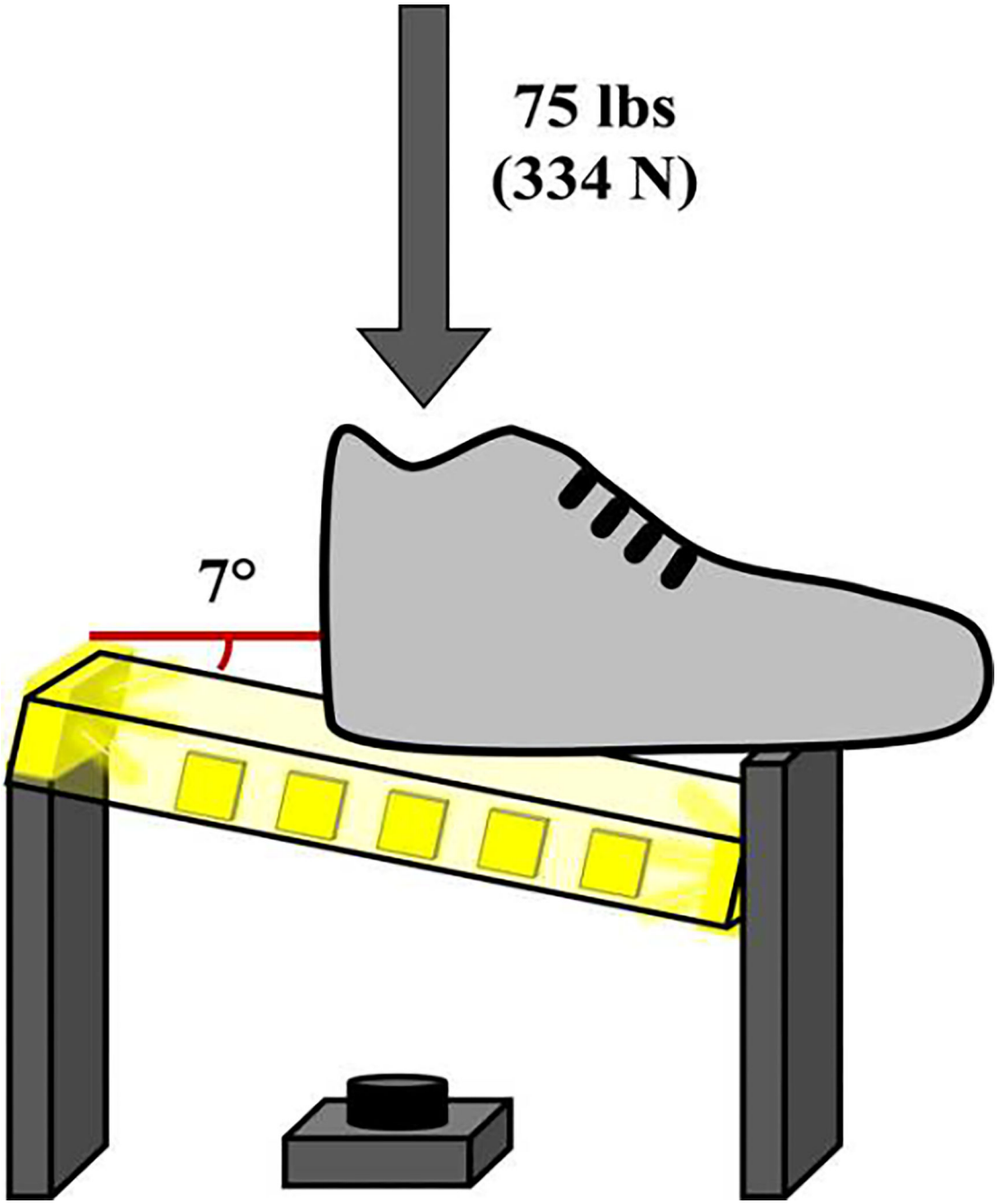

Figure 2.
Setup for shoes on scanner. Shoes were tilted relative to the long axis of the foot to ensure the worn region was in contact during *WornSlip* and using 0° tilt during *NewSlip*. The waveguide was angled at 7° relative to the sagittal plane progression angle of the shoe.

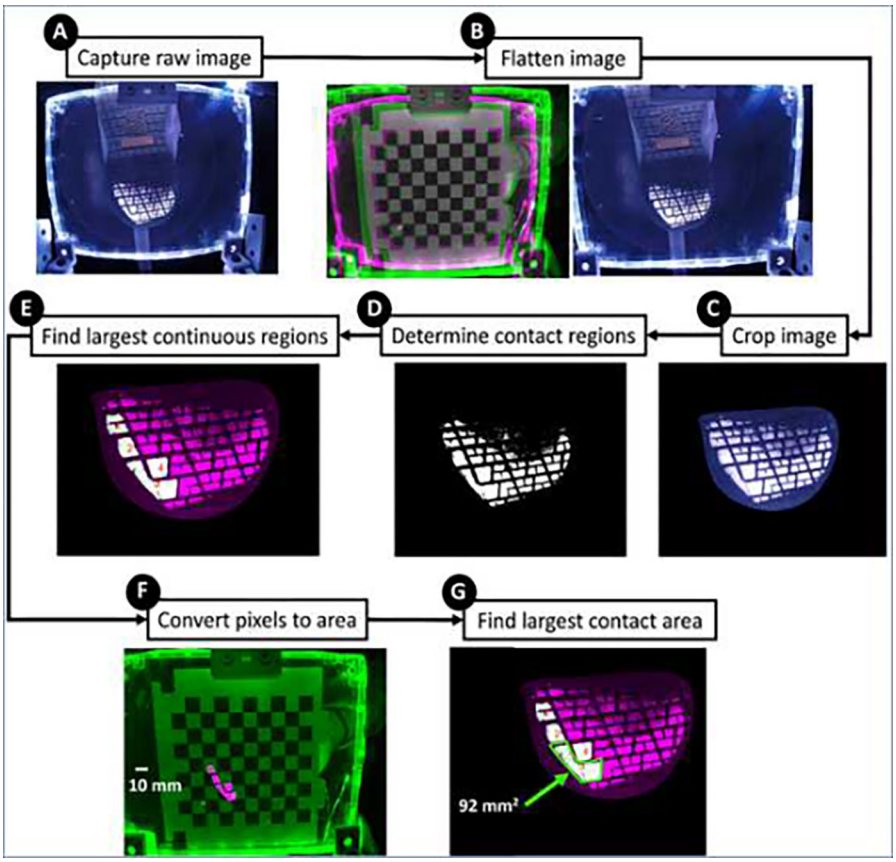

Figure 3.

Image Processing Flowchart for WRS

The raw image (A) was flattened (B) via a calibration technique involving a checkerboard. The image was cropped (C) to select only the regions of the shoe in contact. These regions were then isolated to determine the contact regions (D) and the largest continuous regions were identified (E). The location of the four largest continuous regions were used to determine the pixel-size conversion (F). This conversion was then applied to the largest continuous regions to obtain the largest contact area (G).

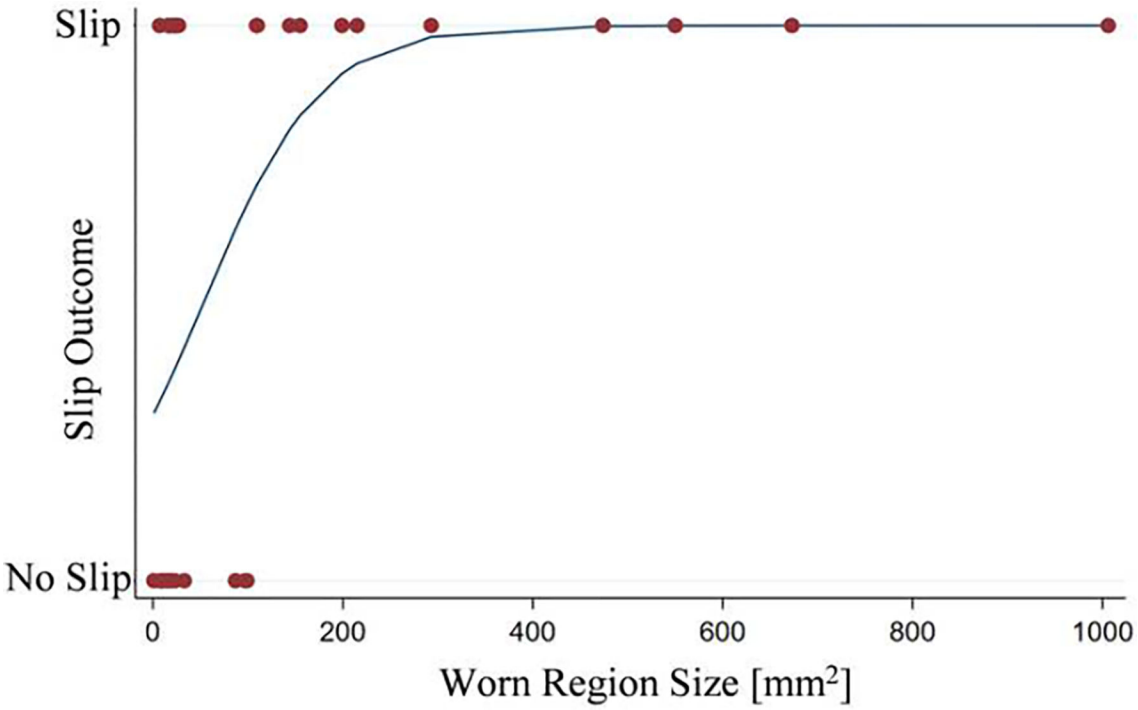

Figure 4.

Slip Outcome vs. WRS – *WornSlip*

The logistic regression for the worn shoes in *WornSlip* is shown with slip outcome on the y-axis and WRS on the x-axis.

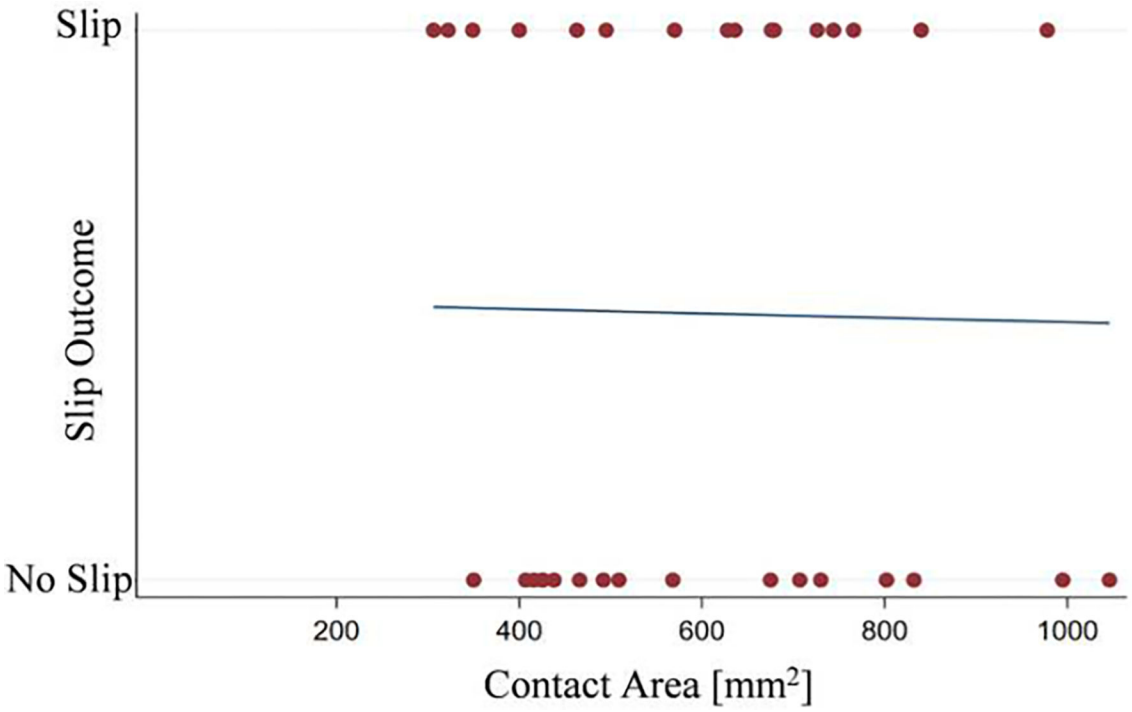

Figure 5.

Slip Outcome vs. CA – *NewSlip*

The logistic regression for the new shoes in *NewSlip* is shown with slip outcome on the y-axis and CA on the x-axis.

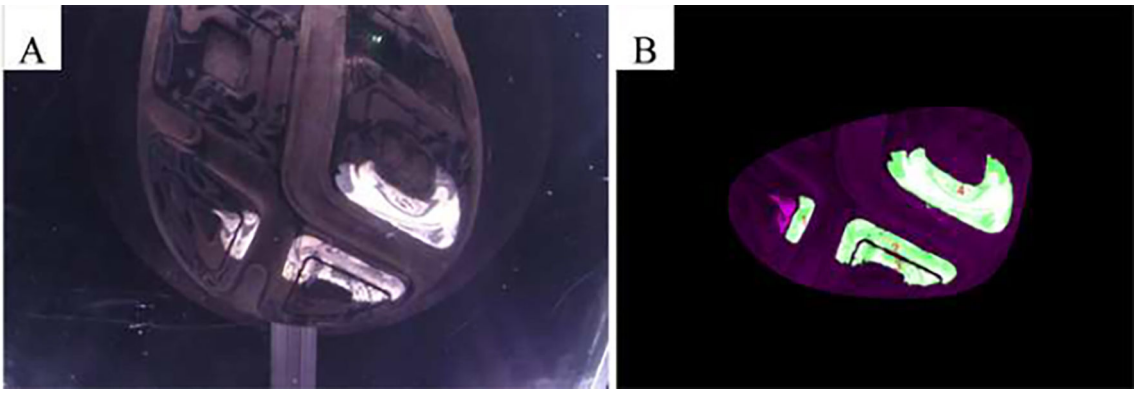

Figure 6.

Shoe Scan – Multi-colored tread

A) Raw scan on tool of shoe with white and black, marbled tread at 17°. B) Image processing of contact region detection using automated selection. Bright white and green tread indicate four largest contact regions detected within image processing.

Table 1.

Measured Worn Region Size (WRS) and Total Contact Area (CA) The mean (standard deviation) and range (in italics) are shown for the WRS (*WornSlip*) and the CA (*NewSlip*). Results are also shown segregated by slip outcome.

	***WornSlip* - WRS [mm^2]**	***NewSlip* - CA [mm^2]**
Mean (SD)	133.4 (224.3)	601.9 (203.0)
Range	*1.0–1006.0*	*306.0–1046.0*
Mean (SD) for slips	214.8 (274.8)	598.6 (196.0)
Range for slips	*7.0–1006.0*	*306.0–978.0*
Mean (SD) for no slips	30.3 (34.0)	604.9 (215.5)
Range for no slips	*1.0–99.0*	*350.0–1046.0*
Slip outcome occurrence (slip/no slip)	19/15	16/17

Table 2.

Worn Region Size (WRS) values per slip risk percentage when using the FTIR (present study) and calipers (Sundaram, et al., 2020)

Slip Risk	WRS [mm^2]	
	FTIR	*Caliper*
50%	39	365
80%	136	1089
95%	331	2342